Environmental Influences on Dark Matter Halos and Consequences for the Galaxies Within Them

Gerard Lemson[1] & Guinevere Kauffmann[2]

[1] *Racah Institute of Physics, The Hebrew University, Jerusalem 91904, Israel*
[2] *Max-Planck Institut für Astrophysik, D-85740 Garching, Germany*

Abstract

We use large N-body simulations of dissipationless gravitational clustering in cold dark matter (CDM) cosmologies to study whether the properties of dark matter halos are affected by their environment. We look for correlations between the masses, formation redshifts, concentrations, shapes and spins of halos and the overdensity of their local environment. We also look for correlations of these quantities with the local tidal field. Our conclusion is extremely simple. Only the mass distribution varies as a function of environment. This variation is well described by a simple analytic formula based on the conditional Press-Schechter theory. We find no significant dependence of any other halo property on environment. Our results do not depend on our choice of cosmology. According to current hierarchical models, the structure and evolutionary history of a galaxy is fully determined by the structure and evolutionary history of the dark halo in which it is embedded. If these models are correct, clustering variations between galaxies of differing morphological types, luminosities, colours and surface brightnesses, must all arise because the halo mass function is skewed towards high mass objects in overdense regions of the Universe and towards low mass objects in underdense regions.

Keywords: galaxies:haloes; galaxies:formation; galaxies:evolution; cosmology:theory; cosmology:dark matter

1 Introduction

It is well known that many of the observed properties of galaxies correlate with their environment. The most famous of these correlations is the morphology-density relation. Davis & Geller (1976) showed that elliptical galaxies are more strongly clustered on the sky than spirals, and Dressler (1980) demonstrated that the elliptical fraction in galaxy clusters is an increasing function of local density. The dependence of the clustering of galaxies on luminosity has been much more controversial, but recent analyses of the largest available redshift surveys confirm that L_* and brighter galaxies have a higher clustering amplitude than low-luminosity galaxies (Park et al 1994; Loveday et al 1995; Benoist et al 1996; Valotto & Lambas 1997). Low surface brightness galaxies are also distributed differently from their high surface brightness counterparts. They are less clustered on all scales (Mo, McGaugh & Bothun 1994) and are particularly isolated on scales smaller than a few Mpc (Bothun et al 1993). Finally, the star formation histories and the gas fractions of galaxies of nominally the same Hubble type are influenced by their local environments. Spiral galaxies in dense environments have redder colours and lower star formation rates that spirals in the field, and often also exhibit truncated HI disks (e.g. Kennicutt 1983; Cayette et al 1994).

One popular hypothesis for the origin of clustering differences between galaxies of different types is that mergers, tidal encounters or interactions with a surrounding gaseous medium modify galaxy properties. Such interactions are more probable in high-density environments. It should be noted, however, that differences in the clustering amplitude of galaxies of different morphologies, luminosities and surface brightnesses persist out to scales where the crossing time is much larger than the Hubble time (Mo et al 1992; Mo, McGaugh & Bothun 1994), so it does appear that galaxies bear some imprint of the initial field of density fluctuations in the Universe.

According to the standard cosmological paradigm, structure in the Universe is built up through a process of hierarchical clustering. Small-scale fluctuations in the initial density field are the first to collapse to form bound, virialized objects (or *dark matter halos*) and these merge together over time to form more and more massive systems. Galaxies form when gas cools, settles, and turns into stars at the centres of the halos (White & Rees 1978; White & Frenk 1991). Galaxy formation models of this type have met with considerable success in explaining many of the trends seen in the properties of galaxies, both at present day and at high redshift (e.g. Lacey et al 1993; Kauffmann, White & Guiderdoni 1993; Cole et al 1994). Their most serious weakness arises from the fact that star formation and supernova feedback processes are poorly understood and hence difficult to model in a convincing way.

It should be noted, however, that one *fundamental* aspect of this picture is that the structure and evolutionary history of a galaxy is *fully determined* by the structure and evolutionary history of its surrounding dark matter halo. The merging history of the halo determines the rate at which gas will cool and become available for star formation, as well as the frequency of merging events and the mass distribution of accreted objects. The density profile of the halo, its shape and its distribution of angular momentum determine the structure, the size and the rotation curve of the galaxy that forms at its centre (Dalcanton, Spergel & Summers 1997; Mo, Mao & White 1997). If the properties of galaxies are observed to vary as a function of environment, it follows that the properties of their surrounding halos must also vary with environment. By understanding exactly which halo properties can be affected by local condi-

tions, one can hope to gain a deeper understanding of the origin of the clustering differences discussed above.

In this paper, we use numerical simulations of gravitational clustering to study the properties of dark matter halos as a function of local density. In order to achieve both good statistics and an accurate treatment of the formation history and internal structure of halos, high resolution simulations are needed, which nevertheless contain a fair sample of the Universe, thus accounting correctly for the influence of large-scale structure on the formation of the halos. We look for correlations between a set of present-day halo properties, including their masses, formation redshifts, concentrations, shapes and spins, with the overdensity of their local environment. We also look for correlations of these quantities with the surrounding tidal field. Our conclusion is extremely simple. Only the mass distribution of dark halos varies as a function of environment. The variation in the mass function is described extremely well by a simple analytic formula based on the conditional Press-Schechter theory derived by Mo & White (1996). We find no significant dependence of any other halo property on environment. Our results do not depend on our choice of cosmology. This leads to the conclusion that the dependences of galaxy morphology, luminosity, surface brightness and star formation rate on environment, must *all* arise because galaxies are preferentially found in higher mass halos in overdense environments and in lower mass halos in underdense environments.

2 The simulations

The GIF project is a joint effort of astrophysicists from Germany and Israel. Its primary goal is to study the formation and evolution of galaxies in a cosmological context using semi-analytical galaxy formation models embedded in large high-resolution N-body simulations. This is done by constructing merger trees of particle halos from dark-matter only simulations and placing galaxies into them using a phenomenological modelling (for a detailed description of this procedure as well as results cf. Kauffmann et al. 1997).

The code used for the GIF simulations is called Hydra. It is a parallel adaptive particle-particle particle-mesh ($\mathrm{AP^3M}$) code (for details on the code cf. Couchman, Thomas, & Pearce 1995; Pearce & Couchman 1997). The current version was developed as part of the VIRGO supercomputing project and was kindly made available by them for the GIF project. The simulations were started on the CRAY T3D at the Computer Centre of the Max-Planck Society in Garching (RZG) on 128 processors. Once the clustering strength required an even larger amount of total memory, they were transferred to the T3D at the Edinburgh Parallel Computer Centre (EPCC) and finished on 256 processors.

A set of four simulations with $N = 256^3$ and with different cosmological parameters was run. In this paper we focus on a variant of a cold dark matter model, τCDM, with $\Omega_0 = 1$, $h = 0.5$, $\sigma_8 = 0.6$ and shape parameter $\Gamma = 0.21$. A value of $\Gamma = 0.21$ is usually preferred by analyses of galaxy clustering, cf. Peacock & Dodds (1994). This is achieved in the τCDM model despite $\Omega_0 = 1$ and $h = 0.5$ by assuming that a massive neutrino (usually taken to be the τ neutrino) had existed during the very early evolution of the Universe and came to dominate the energy density for a short period. It then decayed into lighter neutrinos which are still relativistic, thus delaying the epoch when matter again started to dominate over radiation. The neutrino mass and lifetime are chosen such that $\Gamma = 0.21$. For a detailed

description of such a model see White, Gelmini, & Silk (1995). The normalization was chosen so as to match the abundance of rich clusters (White et al 1993). The simulation box size was 85 h^{-1} Mpc and the particle mass was $2 \times 10^{10} M_{\odot}$. In order to be sure that our results are not sensitive to our choice of cosmological initial conditions, we have also analyzed a low-density CDM model with $\Omega_0 = 0.3$, $\Omega_\Lambda = 0.7$, $\Gamma = 0.21$, h=0.7 and $\sigma_8 = 0.9$ (ΛCDM). This simulation has a somewhat larger box size (141 h^{-1} Mpc), but the same particle mass.

3 Procedure

Halos were selected from the $z = 0$ output times in the simulations as follows. First, we searched for high-density regions using a standard friends-of-friends groupfinder with a linking length of $b = 0.2$ times the mean interparticle separation. We then searched for the particle with the lowest potential energy and adopted its position as the halo centre. The distances of all the particles to the centre were ordered and the radius of the largest sphere with an overdensity $\delta \geq 200$ was defined to be the *virial radius* of the halo, and the mass contained within this radius was defined to be the *virial mass*. Halos were only included in our analysis if the friends-of-friends mass exceeded 70 particles and the virial mass was between 35% and 95% of the friends-of-friends mass. The upper bound served as a check that the majority of particles at overdensities greater than $\simeq 200$ were located by the groupfinder. The lower bound was chosen to ensure that enough particles were located within the virialized region so that the various halo quantities could be calculated reliably.

The following quantities were evaluated for each halo:

1. The spin parameter $\lambda = LE^{1/2}/GM^{5/2}$, calculated for the particles within the virial radius, where L and E are the angular momentum and the thermal kinetic energy of the halo.

2. The formation redshift z_{form}, defined as the redshift at which the most massive halo progenitor was half the present-day mass of the halo.

3. Concentration indices $c_{10} = r_{10}/r_{vir}$ and $c_{20} = r_{20}/r_{vir}$, where r_{10} and r_{20} are the radii enclosing one tenth and one twentieth of the virial mass respectively. These parameters provide a coarse measure of the shape of the density profile of the halo.

4. The shape of the halo was determined by diagonalizing the moment of inertia tensor of halo particles within the virial radius. This gives the principal axes $p_1 \geq p_2 \geq p_3$.

The properties of the local environment around each halo were determined as follows. We evaluated the overdensity δ in spheres of various radii surrounding the halo. We also calculated overdensities in shells around the halo, thereby excluding the contribution of the halo mass itself.

In order to obtain a measure of the higher order harmonics of the surrounding dark matter distribution, a density field on a 128^3 grid (cell size 0.66 h^{-1} Mpc) was obtained from the simulation using cloud-in-cell (CIC) interpolation. The resulting field was smoothed using a top-hat smoothing window of 10 h^{-1} Mpc and the first and second-order spatial derivatives of the density and potential fields were determined using fast Fourier transforms in k-space. We made use of the following k-space window functions:

- density dipole: ik_i
- density shear field: $-k_ik_j$
- potential dipole field (acceleration): $-ik_i/k^2$
- potential shear field (tidal field): k_ik_j/k^2

The resulting fields were interpolated to the positions of the halos using the CIC method. The shear fields were diagonalized and the eigenvalues ordered.

4 Results

4.1 The mass function of halos versus environment

In an extension of the Press-Schechter theory, Bond et al (1991) and Bower (1991) derive an expression for the fraction of mass in a region of initial radius R_0 and linear overdensity δ_0, which at redshift z_1 is contained in halos of mass M_1. If one assumes that the region R_0 evolves in size and overdensity according to the spherical top-hat collapse model, it is simple to derive a formula for the mass function of halos in a present-day region of radius R and overdensity δ. This was first done by Mo & White (1996). They tested their analytic formula against results from N-body simulations containing 128^3 particles.

In figure 1, we show how the shape of the halo mass function changes as a function of local overdensity δ evaluated within spheres of R= 10 h^{-1} Mpc. The thick solid line shows results derived from the τCDM simulation at $z = 0$. The thin solid line shows the analytic prediction of Mo & White (1996). For comparison, the thick dashed line is the *average* halo mass function evaluated from the simulation, multiplied by a factor $(1 + \delta)$. The thin dashed line is the same quantity calculated from the Press-Schechter theory. For clarity, the simulation and the analytic curves have been offset by 1 decade in the y-direction.

Although it is not apparent as a result of the way we have chosen to present our results, it should be noted that the halo abundances predicted by the analytic theory exceed those derived from the simulation by a factor $\simeq 1.5$ over the range of halo masses shown in figure 1. The magnitude of this offset is in rough agreement with that found by Lacey & Cole (1994) in their tests of the Press-Schechter formalism. Nevertheless, as can be seen in the plot, the theory does predict the change in shape of the halo mass function with δ remarkably well. As can be seen, in low density regions, high-mass halos are underepresented, whereas in high-density regions the situation is reversed and high-mass halos are overabundant.

4.2 Formation times, Spins, Concentrations and Shapes of Halos

Our principal result is that we find *no correlation* between the environment of halos and their formation times, spins, concentrations and shapes in either the τCDM or the ΛCDM simulations. Out of a large number of possible scatterplots, we have selected the following few to illustrate this conclusion. Results are shown only for the τCDM model, but plots for ΛCDM are virtually identical.

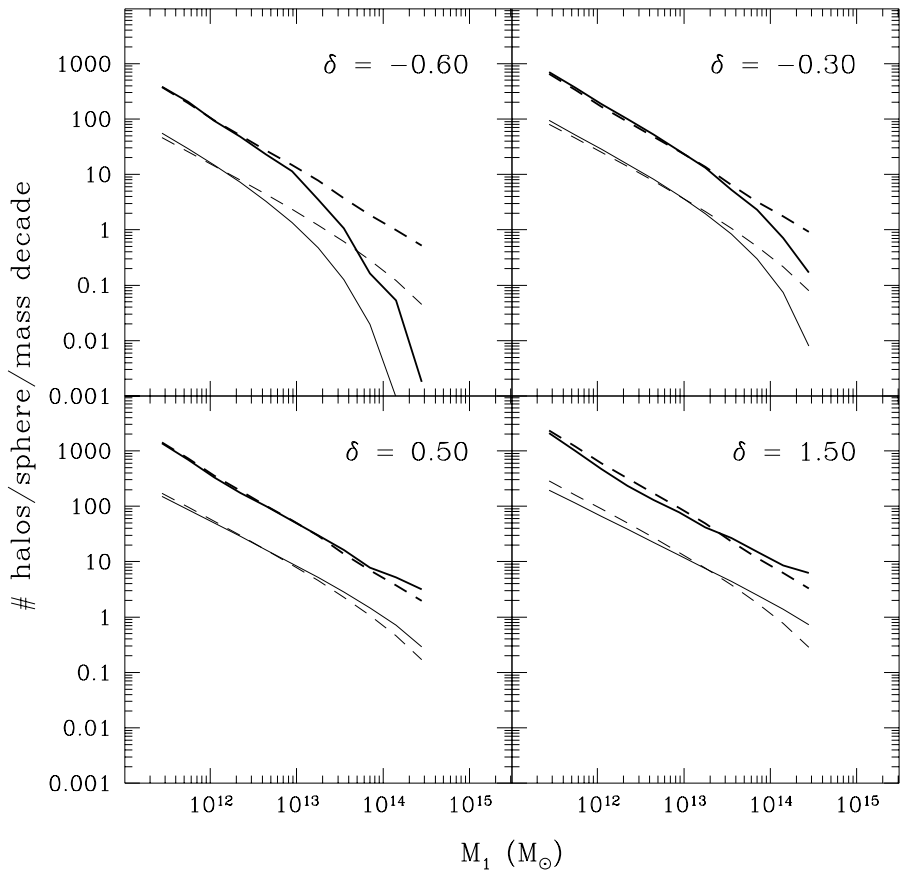

Figure 1: The halo mass function in spheres of radius R=10 h^{-1} Mpc and local overdensity δ. The thick solid line shows results derived from the τCDM simulation at $z = 0$. The thin solid line shows the analytic prediction of Mo & White (1996). For comparison, the thick dashed line is the *average* halo mass function evaluated from the simulation, multiplied by a factor $(1 + \delta)$. The thin dashed line is the same quantity calculated from the Press-Schechter theory. For clarity, the simulation and the analytic curves have been offset by 1 decade in the y-direction.

In figure 2 we plot the value of the spin parameter λ against the overdensity in top-hat spheres of radius 10 h^{-1} Mpc for halos in four different mass bins. This figure shows that the mean value of λ varies at most very weakly with overdensity or with mass. There does appear to be a slight tendency for λ to increase with overdensity. These results do not change if we adopt a different value of the smoothing radius.

In figure 3 we plot formation redshift against the overdensity in a shell between 2 h^{-1} and 5 h^{-1} Mpc surrounding each halo. No dependence of mean formation redshift on overdensity is seen. Higher mass halos form somewhat later on average, as expected (Lacey & Cole 1993).

Figures 2 and 3 demonstrate that the *average* spin and formation time of halos are not correlated with their environments. The next step is to demonstrate that the full probability distributions are also independent of local overdensity. This is shown in figure 4, where we plot $P(\lambda)$ and $P(z_{form})$, for three different ranges in overdensity δ. As can be seen, the curves are almost indistinguishable from each other. Again, there is perhaps a slight shift towards larger spins in overdense regions. The distribution of λ is consistent with that found in earlier work (e.g. Barnes & Efstathiou 1987).

Finally, figure 5 is a mosaic illustrating a further subset of the possibilities we have explored. In the two left panels, we show the concentration index c_{10} versus the overdensity evaluated in spheres of radius 10 h^{-1} Mpc surrounding each halo, and the shape axis ratio p_1/p_3 versus the tidal field axis ratio ($\phi_{,11}/\phi_{,33}$). In the two right panels, we plot the spin parameter and the formation redshift versus principal axes ratios of the tidal field and the density shear field respectively. (Note that the apparent gaps in the distribution of λ and p_1/p_3 at small positive values of $\phi_{,11}/\phi_{,33}$ result from the ordering of the eigenvalues and the values that the $\phi_{,ii}$ assume in practice.) Once again, no correlations are found, either in the mean values of the halo quantities, or in their full probability distributions. It is interesting that neither the spins, nor the distribution of shapes of dark halos, depend on the surrounding tidal field.

5 Discussion and Conclusions

In this paper, we have demonstrated that mass is the only halo property that correlates significantly with local environment. The dependence of the halo mass function on environment can be understood in terms of a simple extension of the Press-Schechter theory.

It is interesting to note that the fact that halo formation histories do not depend on local overdensity, is a prediction of the extended Press-Schechter theory in the excursion set formulation of Bond et al (1991). In this approach, the standard formulae are obtained by assuming that the mass of a halo to which any given mass element belongs, can be followed by studying the behaviour of the initial linear density field as it is smoothed with a succession of sharp k-space filters. In this model, the history of each mass element of a halo of mass M (and thus the formation history of the halo itself) is statistically independent of the future of the element and thus of the halo's environment. Navarro, Frenk & White (1996) have demonstrated that the density profile of dark matter halos in CDM-like cosmologies has a "universal" form, and that the characteristic density of a halo is related simply to its formation time. It is thus also not surprising that our concentration parameters c_{10} and c_{20} turn out to be independent of environment. There has also been substantial analytic work concerned with the angular momentum generated by tidal torques acting on local density maxima in the

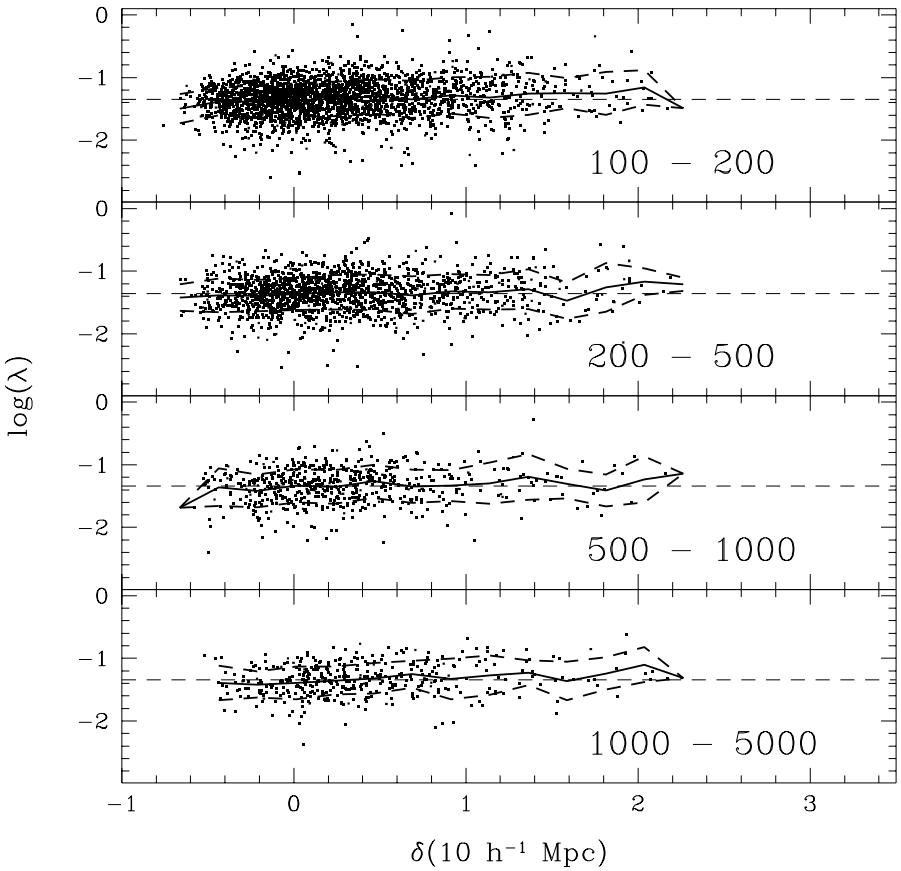

Figure 2: The spin parameter λ is plotted against overdensity in spheres of radius R=10 h^{-1} Mpc for halos in different mass ranges, indicated on each panel as the number of particles found within the virial radius. The solid line shows the mean value of $\log(\lambda)$ as a function of δ. Dashed lines indicate the 1σ standard deviation.

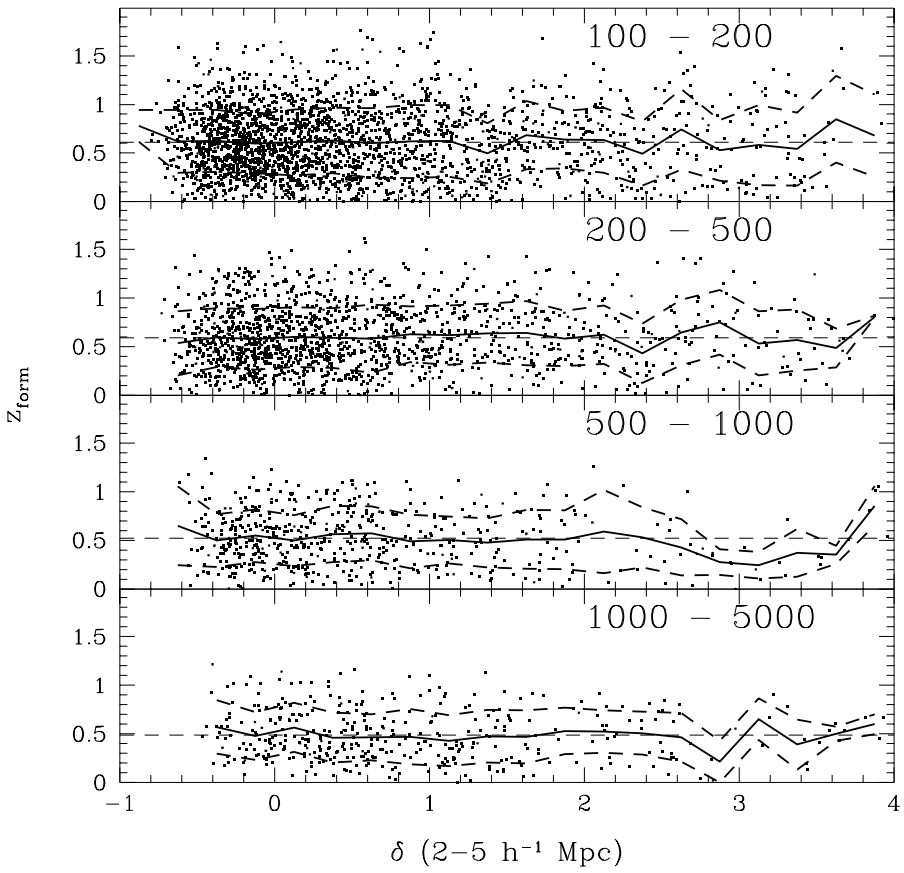

Figure 3: The formation redshift is plotted against overdensity in the shell between 2 and 5 h^{-1} Mpc for halos in different mass ranges. For an explanation of the lines, see figure 2.

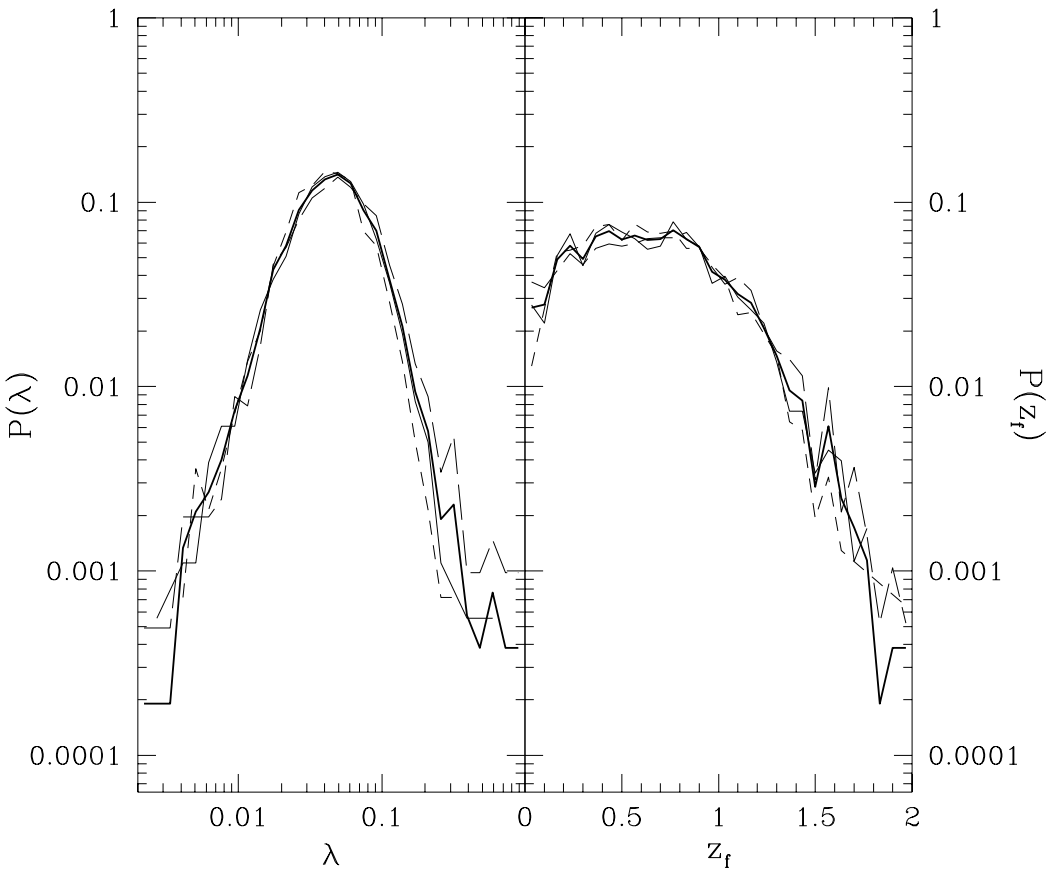

Figure 4: The probability distribution of the spins and the formation redshifts of halos in regions of different overdensity δ. δ is calculated in a 10 h^{-1} Mpc sphere for the left-hand panel, and in a 2-5 h^{-1} Mpc shell for the right-hand panel. The thick solid line in both panels represents the full probability distribution. In the left panel, the short dashed, thin solid, and long-dashed lines are for $-1 < \delta < -0.1$, $-0.1 < \delta < 0.3$, and $0.3 < \delta$. In the right panel, the short dashed, thin solid, and long-dashed lines are for $-1 < \delta < -0.1$, $-0.1 < \delta < 0.6$, and $0.6 < \delta$. Bins in δ have been chosen so that they contain an equal number of haloes.

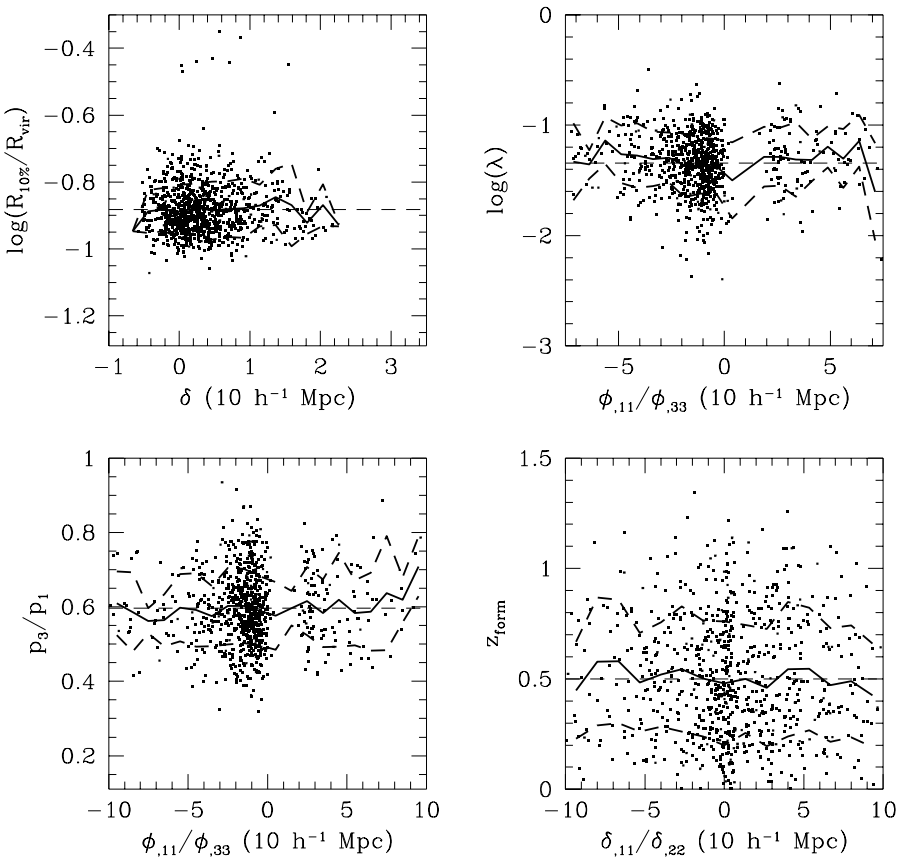

Figure 5: A mosaic of four different correlations between halo properties and environment. The top left panel shows the concentration index ($c_{10} = R_{10}/R_{vir}$) as a function of δ in a sphere. The bottom left panel shows the relationship between the shape axis ratio p_3/p_1 and the the ratio of the first and third eigenvalues of the tidal field. In the top right panel, the spin parameter is plotted against the ratio of the first and third eigenvalues of the tidal field. In the bottom right panel, formation redshift is plotted against the ratio of the first and second eigenvalues of the density shear field. Only halos in the mass range 500-5000 are shown.

linear density field. It has been argued (Blumenthal et al 1984; Hoffman 1986) that the height of a peak is anticorrelated with its angular momentum, on the basis that high peaks collapse early, so there is not much time for tidal torques to act. If this was the case, overdense regions of the Universe, in which high peaks are more probable, should harbor halos with systematically lower angular momentum. Heavens & Peacock (1988) pointed out that this effect is counterbalanced by the fact that higher peaks experience greater tidal torques. For realistic power spectra, they estimate that the two effects should nearly cancel out. Steinmetz & Bartelmann (1995) obtain a similar result by modelling the formation of a halo as a collapse of a homogeneous ellipsoid acted upon by tidal shear from the surrounding matter. Both analyses are consistent with the very weak environment-dependence of spin in our data. The shapes of dark matter halos have proven more difficult to calculate using analytic methods. Dubinski (1992) has investigated halo shapes in high-resolution N-body simulations and finds that there is no relationship between the shape of the initial density peak and the shape of the final collapsed halo. On the other hand, West, Villumsen & Dekel (1991) and Tormen (1997) have demonstrated a clear tendency for the major axis of cluster-sized halos to align with larger-scale structures.

The main astrophysical implication of our conclusion is that clustering differences between galaxies of different types must arise purely because different galaxies sample different mass halos. Semi-analytic models of galaxy formation in hierarchical cosmologies demonstrate that it is possible to explain many of the clustering trends seen in the data in this way (Kauffmann, Nusser & Steinmetz 1997). In these models, elliptical galaxies form when disk galaxies of comparable mass merge with each other. These mergers occur preferentially in groups at redshifts $\simeq 1$. The groups then coalesce to form clusters and superclusters. As shown by Kauffmann, White & Guiderdoni (1993) and Baugh, Cole & Frenk(1996), the fraction of ellipticals increases strongly with halo mass in this picture and ellipticals thus end up more clustered than spirals. In addition, the luminosity of the central galaxy in a halo scales in proportion to the halo mass, simply because more gas is able to cool and form stars in more massive halos. Luminosity-dependent clustering is thus a natural outcome of the models. Finally, it should also be noted that galaxies are assumed to be stripped of their surrounding dark matter once they have been accreted by a larger system, such as a group or cluster. They thus lose their supply of new cold gas, their star formation rates decline, and their stellar populations redden and fade. Red, gas-poor galaxies are thus found predominantly in high mass halos and are again predicted to be more clustered. The semi-analytic models at present provide no explanation for the clustering differences between galaxies of different surface brightnesses. One might speculate that low surface-brightness disks are more fragile and are more easily destroyed in high-density environments. More detailed modelling is necessary, however, before a conclusion can be drawn as to whether this will work in practice.

Acknowledgments

We thank Simon White, Adi Nusser and Joe Silk for helpful discussions.

References

Barnes, J. & Efstathiou, G., 1987, ApJ, 319, 575

Baugh, C.M., Cole, S. & Frenk, C.S., 1996, MNRAS, 283, 1361

Benoist, C., Maurogordato, S., Dacosta, L.N., Cappi, A. & Schaeffer, R., ApJ, 1996 472, 452

Blumenthal, G.R., Faber, S.M., Primack, J.R. & Rees, M.J., 1984, Nature, 311, 517

Bond, J.R., Cole, S., Efstathiou, G. & Kaiser, N. 1991, ApJ, 379, 440

Bothun, G.D., Schombert, J.M., Impey, C.D., Sprayberry, D. & McGaugh, S.S., 1993, AJ, 106, 530

Bower, R.J., 1991, MNRAS, 248, 332

Cayette, V., Kotanyl, C., Balkowski, C. & Van Gorkom, J.H., 1994, AJ, 107, 1003

Cole, S., Aragón-Salamanca, A., Frenk, C.S., Navarro, J.F. & Zepf, S.E., 1994, MNRAS, 271, 781

Couchman, H.M.P., Thomas, P.A. & Pearce, F.R., 1995, ApJ, 452, 797

Dalcanton, J.J., Spergel, D.N. & Summers, F.J., 1997, ApJ, 482, 659

Davis, M. & Geller, M.J., 1976, ApJ, 208, 13

Dressler, A., 1980, ApJ, 237,351

Dubinski, J., 1992, ApJ, 401,441

Heavens, A. & Peacock, J., 1988, MNRAS, 232, 339

Hoffman, Y., 1986, ApJ, 301, 65

Kauffmann, G., White, S.D.M. & Guiderdoni, B. 1993, MNRAS, 264, 201 (KWG)

Kauffmann, G., Nusser, A. & Steinmetz, M., 1997, MNRAS, 286, 795

Kauffmann, G., Diaferio, A., Colberg, J. & White, S.D.M., 1997, in preparation

Kennicutt, R.C. 1983, AJ, 88, 483

Lacey, C., Guiderdono, B., Rocca-Volmerange, B. & Silk, J., 1993, ApJ, 402, 15

Lacey, C. & Cole, S., 1993, MNRAS, 262, 627

Lacey, C. & Cole, S., 1994, MNRAS, 271, 676

Loveday, J., Maddox, S.J., Efstathiou, G. & Peterson, B.A., 1995, ApJ, 442,457

Mo, H.J., Einasto, M., Xia, X.Y. & Deng, Z.G., 1992, MNRAS, 255, 382

Mo, H.J., McGaugh, S.S. & Bothun, G.D., 1994, MNRAS, 267, 129

Mo, H.J. & White, S.D.M., 1996, MNRAS, 282, 347

Mo, H.J., Mao, S. & White, S.D.M., 1997, MNRAS, submitted

Navarro, J.F., Frenk, C.S. & White, S.D.M., 1996, ApJ, 462, 563

Park, C.B., Vogely, M.S., Geller, M.J. & Huchra, J.P., 1994, APJ, 431, 569

Peacock, J.A. & Dodds, S.J., 1994, MNRAS, 267, 1020

Pearce, F.R. & Couchman, H.M.P., 1997, New Astronomy, submitted

Steinmetz, M. & Bartelmann, M., 1995, MNRAS, 272, 570

Tormen, G., 1997, MNRAS, 290, 411

Valotto, C.A. & Lambas, D.G., 1997, ApJ, 481, 594

West, M.J., Villumsen, J.V. & Dekel, A., 1991, ApJ, 369, 287

White, M., Gelmini, G. & Silk, J., 1995, Phys. Rev. D., 51, 2669

White, S.D.M. & Rees, M.J., 1978, MNRAS, 183, 341

White, S.D.M. & Frenk, C.S., 1991, ApJ, 379, 52

White, S.D.M., Efstathiou, G. & Frenk, C.S.,1993, MNRAS, 262, 1023